

## FILTER SOLUTIONS FOR THE NONLINEAR INVERSE HEAT CONDUCTION PROBLEM

James V. Beck, Prof. Em. Dept. of Mech. Eng., Mich. State Univ., East Lansing, MI 48824 and Beck Engineering Consultants Co., Okemos, MI 48864, USA. E-mail: [beck@egr.msu.edu](mailto:beck@egr.msu.edu)

**Abstract** – Estimation of the heat flux for a quenched solid tungsten sphere is demonstrated using a filter formulation. Even though the values of the thermal properties significantly change during quenching, nearly as accurate heat flux estimates as with a temperature-variable analyses are possible using the proposed filter method. The filter algorithm is very efficient for the repeated analyses of similar tests. The filter solution method can utilize several IHCP methods including function specification and Tikhonov regularization.

### 1. INTRODUCTION

The determination of the heat flux at a surface of a body from transient temperature measurements inside the body is called the inverse heat conduction problem, IHCP. The IHCP can be linear or nonlinear depending upon whether the thermal properties are constant or functions of temperature. An efficient method of solution for the linear IHCP uses the filter coefficient method which is described in [2]. The use of the filter coefficient method for nonlinear IHCPs is demonstrated herein and has not been previously described.

The filter solution method for temperature-independent thermal properties is computationally very simple and efficient. The method involves a moving summation such as

$$\hat{q}_M = \sum_{j=1}^{m_p+m_f} f_j Y_{m_f+M-j}, \quad M = m_p + 1, m_p + 2, \dots, j_{\max} - m_f \quad (1)$$

The subscript  $M$  is the time index of the heat flux component (in  $\text{W/m}^2$ ) of interest;  $f_j$  is the  $j$ th filter coefficient ( $\text{W/m}^2\text{-}^\circ\text{C}$ ); and  $Y_{m_f+M-j}$  is the measured temperature ( $^\circ\text{C}$ ) at times including those both before and after the time of interest which is denoted,  $t_M$ . (The “true” or “model” temperature is denoted by the symbol  $T$ .) The indices  $m_p$  and  $m_f$  are for the past and future values, respectively, of the measured temperature;  $j_{\max}$  is the total number of the measurement times. (The index  $M$  also denotes the “first” future time.) A simple example is for the heat flux at the 25<sup>th</sup> time and for  $m_p = 3$  and  $m_f = 2$  so that the heat flux at that time is estimated using

$$\hat{q}_{25} = f_1 Y_{26} + f_2 Y_{25} + f_3 Y_{24} + f_4 Y_{23} + f_5 Y_{22} \quad (2)$$

The “future” temperatures are  $Y_{25}$  and  $Y_{26}$ . The sum of the indices in each product of  $f$  times  $Y$  is equal to  $M - m_f = 27$ . Another point is that the filter coefficients should sum to zero for the herein applications. For nonlinear cases the filter coefficients can vary with the temperature level.

In quenching tests, the same or similar device for heat flux measurement is repeatedly used. In such tests, a machined part or a calorimeter initially at an elevated temperature is plunged into a cold fluid. In other situations, the process is continuous but has a periodic character, such as during casting parts with molten aluminum or forming bottles from molten glass. The filter solution of the nonlinear IHCP is particularly suited for these manufacturing instrumentation tasks because it does not require a beginning or end time in the analysis and also the method is relatively easy to understand and implement after the filter coefficients have been determined.

The method has general applications in monitoring manufacturing processes and analysis of scientific experiments directed toward understanding of boiling, for example. This paper uses an example of quenching a 1 cm diameter tungsten sphere; various modes of boiling can occur during the cooling phase. It is demonstrated herein that the heat flux components in such a case can be accurately estimated using a filter equation analogous to eqn. (1) with the coefficients being only weak functions of temperature, even though the temperatures may go from 1100  $^\circ\text{C}$  down to almost room temperature in just a few seconds.

The use of filter coefficients does not by itself introduce the required regularization [2] in the estimation of the heat flux. Instead the filter coefficients are generated with some method which incorporates regularization. Function specification [2] and Tikhonov regularization [2, 7] are possible methods as is mollification [5]. A method which transforms the linear IHCP into a nonlinear problem may not be used, such as when the conjugate gradient method is incorporated in the solution.

The transient heat conduction equation for the sphere can be solved in any appropriate manner including finite elements, finite control volumes and exact methods of solution. The latter is shown to be possible in the example described below. Also inaccuracies in the thermal properties and errors in the temperature measurements [1] may not be compatible with an extremely accurate  $T$ -variable model for determining the filter coefficients. For these reasons, an analytical solution is employed in the direct solution.

## 2. DIRECT PROBLEM

The direct problem can be described with a heat conduction model of a sphere of radius  $b$  which is

$$\frac{k}{r^2} \frac{\partial}{\partial r} \left( r^2 \frac{\partial T}{\partial r} \right) = C \frac{\partial T}{\partial t}, \quad 0 < r < b, \quad t > 0 \quad (3)$$

which incorporates the assumption of the thermal conductivity,  $k$ , being independent of the model temperature  $T$ . The volumetric heat capacity,  $C$ , is also considered to be constant in the analysis. As will be demonstrated, the thermal properties can be assigned a series of constant values as the problem progresses. The initial temperature is assumed to be the constant  $T_0$  and the boundary conditions can be given by

$$T(0, t) = \text{finite}, \quad k \frac{\partial T}{\partial r}(b, t) = q(t) \quad (4)$$

By giving the heat flux in this manner, the heat flux  $q(t)$  is positive when the sphere is heated and negative when cooled. The temperature at center ( $r = 0$ ) is measured at discrete times with uniform time steps,

$$Y_i \approx T(0, i\Delta t), \quad i = 1, 2, \dots, j_{\max} \quad (5)$$

which is used to determine the heat flux at the outer radius  $b$  of the sphere.

Before discussing the inverse problem, the temperature solutions for two direct problems for the sphere with 1) constant (or square) and 2) triangular heat flux basis functions. Consider first the case of approximating transient heat flux histories with the piece-wise constant basis functions,

$$i^{\text{th}} \text{ piece-wise constant heat flux basis function} = q_i, \quad t_{i-1} < t < t_i, \quad i = 1, 2, \dots, j_{\max} \quad (6)$$

Using the principle of superposition as expressed by Duhamel's integral, eqn. (3.2.12) of [2] gives the temperature at time  $t_M = M\Delta t$  by

$$T_M = T_0 + \sum_{i=1}^M q_i \Delta \phi_{M-i}, \quad \Delta \phi_i = \phi_{i+1} - \phi_i, \quad \Delta \phi_0 = \phi_1 - \phi_0 = \phi_1 \quad (7)$$

where  $\phi_i$  is the temperature at  $r = 0$  and time  $t_i$  for the heat flux  $q_0$  equal to unity (i.e.,  $q_0 = 1$ ). An analytical expression for the temperature in a sphere with a constant heat flux is [3, p. 272]

$$\frac{T(r, t) - T_0}{q_0 b / k} = 3 \frac{\alpha t}{b^2} + \frac{1}{2} \left( \frac{r}{b} \right)^2 - \frac{3}{10} - 2 \frac{b}{r} \sum_{m=1}^{\infty} \frac{1}{\beta_m^2} e^{-\beta_m^2 \frac{\alpha t}{b^2}} \frac{\sin\left(\beta_m \frac{r}{b}\right)}{\sin(\beta_m)} \quad (8a)$$

At the center of the sphere this expression yields

$$\frac{T(0, t) - T_0}{q_0 b / k} = 3 \frac{\alpha t}{b^2} - \frac{3}{10} - 2 \sum_{m=1}^{\infty} \frac{1}{\beta_m} e^{-\beta_m^2 \frac{\alpha t}{b^2}} \frac{1}{\sin(\beta_m)} \quad (8b)$$

The eigenvalues are found from the transcendental equation,  $\tan(\beta_m) = \beta_m$ . Using the notation given in [3, Chap. 2], this problem is denoted *RS02B1T0* where "RS" denotes the radial spherical coordinate, "02" denotes the finite  $T$  condition at  $r = 0$  and a heat flux boundary condition at  $r = b$ , B1 denotes a boundary condition of a constant heat flux and T0 denotes a zero initial temperature. The upper two curves in Figure 1 are for this *RS02B1T0* problem; the temperature at  $r = 0$  is nearly zero until  $\alpha t / b^2 = 0.04$  when this temperature rise eventually reaches 0.03% that of the surface at that time.

Another function for approximating a curve uses linearly time-varying elements. Analogous to eqn. (6) we now can use triangular basis function which is equal to zero everywhere except in the ranges given by

$$i^{\text{th}} \text{ triangular heat flux basis function} = \begin{cases} q_i \frac{t - t_{i-1}}{\Delta t}, & t_{i-1} < t < t_i \\ q_i \frac{t_i - t}{\Delta t}, & t_i < t < t_{i+1} \end{cases} \quad (9)$$

This basis function requires the solution for a linearly increasing heat flux which can be written as

$$\frac{T(r, t)}{\frac{q_0 b}{k} \frac{\alpha t_0}{b^2}} = \frac{3}{2} \left( \frac{\alpha t}{b^2} \right)^2 + \frac{\alpha t}{b^2} \left[ \frac{1}{2} \left( \frac{r}{b} \right)^2 - \frac{3}{10} \right] + \frac{1}{40} \left( \frac{r}{b} \right)^4 - \frac{1}{20} \left( \frac{r}{b} \right)^2 + \frac{27}{1400} + 2 \frac{b}{r} \sum_{m=1}^{\infty} \frac{1}{\beta_m^4} e^{-\beta_m^2 \frac{\alpha t}{b^2}} \frac{\sin\left(\beta_m \frac{r}{b}\right)}{\sin(\beta_m)} \quad (10a)$$

At the center of the sphere, eqn. (10a) yields

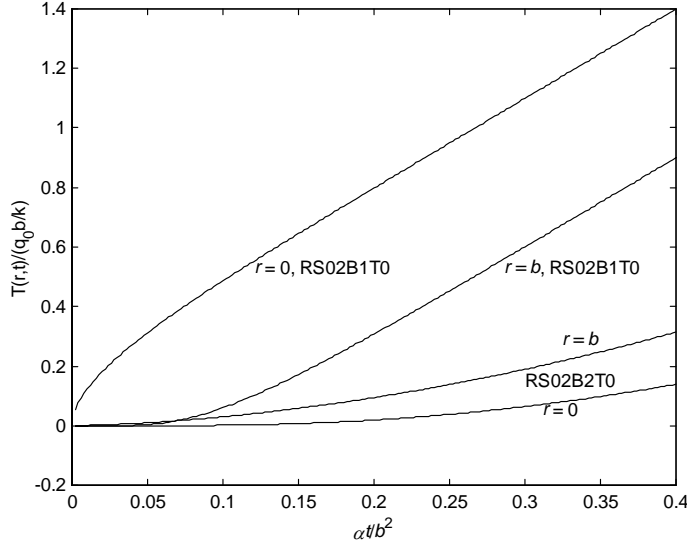


Figure 1. Temperatures in a solid sphere with a constant heat flux at  $r = b$  (denoted *RS02B1T0*) and a linearly increasing heat flux (denoted *RS02B2T0*).

$$\frac{T(0,t)}{q_0 b} \frac{b^2}{k \alpha t_0} = \frac{3}{2} \left( \frac{\alpha t}{b^2} \right)^2 - \frac{3}{10} \frac{\alpha t}{b^2} + \frac{27}{1400} + 2 \sum_{m=1}^{\infty} \frac{1}{\beta_m^3} e^{-\beta_m^2 \frac{\alpha t}{b^2}} \frac{1}{\sin(\beta_m)} \quad (10b)$$

This solution is denoted *RS02B2T0* where the “B2” denotes a heat flux that varies linearly with time. Plots of eqn. (10a,b) for  $r = 0$  and  $b$  are given in Figure 1; see the lowest two curves which are for  $b^2 / \alpha t_0 = 1$ . Notice that the derivative of eqns (10a,b) with respect to  $t/t_0$  yields eqns (8a,b), which is referenced below.

### 3. INVERSE HEAT CONDUCTION ALGORITHMS

#### 3.1 Function Specification: Constant heat flux basis functions

One type of inverse heat conduction algorithm uses a temporary functional form of the future heat fluxes. For the heat flux being constant, (that is, using piece-wise constant basis functions) for the  $r_f$  future times  $t_M, t_{M+1}, \dots, t_{M+r_f-1}$ , the estimated heat flux at time  $t_M$  is (see eqn. (7) and [2, eqn. (4.4.24)])

$$\hat{q}_M = \left[ \sum_{i=1}^{r_f} \left( Y_{M+i-1} - \hat{T}_{M+i-1} \Big|_{q_M = \dots = 0} \right) \phi_i \right] \left[ \sum_{i=1}^{r_f} \phi_i^2 \right]^{-1} \quad (11)$$

This estimated heat flux  $\hat{q}_M$  is best associated with the time of  $t_{M-1/2}$ .

#### 3.2 Function Specification: Triangular heat flux basis functions

Now let us consider the case of the triangular basis functions which implies that the heat flux varies with linear segments such that

$$q = 0 \text{ at } t = 0, \quad q = q_1 \text{ at } t_1, \quad q = q_2 \text{ at } t_2, \quad q = q_3 \text{ at } t_3, \dots, q = q_i \text{ at } t_i = i\Delta t \quad (12)$$

For the time period of  $t_i < t < t_{i+1}$ , the heat flux varies linearly in time such as

$$q = q_i + (q_{i+1} - q_i) \frac{t - t_i}{\Delta t} \quad (13)$$

Let  $\eta_i$  be equal to the temperature  $T$  at the center,  $r = 0$ , and at time  $t_i$  for a linearly increasing heat flux. Specifically let  $\eta_1$  be the temperature at time  $t_1 = \Delta t$  for the heat flux  $q_1 = 1$ ; also let  $\eta_2$  be the temperature at time  $t_2$  for the heat flux  $q_2 = 2$  at  $t_1 = 2\Delta t$  and  $q_1 = 1$ . Then explicitly we have

$$\eta_1 = T(0, \Delta t) \Big|_{q_1=1}, \quad \eta_2 = T(0, 2\Delta t) \Big|_{q_1=1, q_2=2}, \quad \eta_i = T(0, i\Delta t) \Big|_{q_1=1, q_2=2, \dots, q_i=i} \quad (14)$$

The temperature at  $t_i, i = 1, 2, \dots$  is (using triangular basis functions and assuming the initial  $T_0 = 0$ )

$$\begin{aligned}
 T_1 &= q_1 \eta_1 = q_1 (\eta_{-1} - 2\eta_0 + \eta_1) = q_1 \delta^2 \eta_0 \\
 T_2 &= q_1 (\eta_0 - 2\eta_1 + \eta_2) + q_2 (\eta_{-1} - 2\eta_0 + \eta_1) = q_1 \delta^2 \eta_1 + q_2 \delta^2 \eta_0 \\
 &\vdots \\
 T_M &= \sum_{i=1}^M q_i \delta^2 \eta_{M-i}
 \end{aligned} \tag{15}$$

$$\delta^2 \eta_0 = \eta_1, \quad \delta^2 \eta_i = \eta_{i-1} - 2\eta_i + \eta_{i+1}, \quad i = 1, 2, \dots \tag{16}$$

Now the objective is to express the temperature at times  $M, M + 1, M + 2, \dots, M + r_f - 1$  in terms of the heat fluxes at times  $M - 1$  and  $M$ . The temporary assumption is that the heat flux is varying in a linear fashion starting at time  $t_{M-1}$ . The results are

$$\begin{aligned}
 T_M &= \sum_{i=1}^{M-1} q_i \delta^2 \eta_{M-i} + q_M \delta^2 \eta_0 = \sum_{i=1}^{M-1} q_i \delta^2 \eta_{M-i} + q_M \eta_1 \\
 T_{M+1} &= \sum_{i=1}^{M-1} q_i \delta^2 \eta_{M+1-i} + q_M \delta^2 \eta_1 + q_{M+1} \delta^2 \eta_0 = \sum_{i=1}^{M-1} q_i \delta^2 \eta_{M+1-i} + q_M \eta_2 - q_{M-1} \eta_1 \\
 &\vdots \\
 T_{M+j} &= \sum_{i=1}^{M-1} q_i \delta^2 \eta_{M+j-i} + q_M \eta_{j+1} - q_{M-1} \eta_j
 \end{aligned} \tag{17}$$

To find the estimate of  $q_M$ , we minimize with respect to  $q_M$  the sum of squares function

$$S = \sum_{k=1}^{r_f} \left( Y_{M+k-1} - \sum_{i=1}^{M-1} q_i \delta^2 \eta_{M+k-1-i} - q_M \eta_k + q_{M-1} \eta_{k-1} \right)^2 \tag{18}$$

Taking the first derivative of  $S$  with respect to  $q_M$ , etc. gives the triangular basis function heat flux estimator

$$\hat{q}_M = \left[ \sum_{k=1}^{r_f} \left( Y_{M+k-1} - \sum_{i=1}^{M-1} q_i \delta^2 \eta_{M+k-1-i} + q_{M-1} \eta_{k-1} \right) \eta_k \right] \left[ \sum_{k=1}^{r_f} \eta_k^2 \right]^{-1} \tag{19}$$

Both the piece-wise constant and triangular basis function representations for temperature given above, eqns (7) and (15), can be described by the matrix equation of

$$\mathbf{T} = \mathbf{X} \mathbf{q} \tag{20}$$

where

$$\mathbf{T} = \begin{bmatrix} T_1 \\ T_2 \\ \vdots \\ T_n \end{bmatrix}, \quad \mathbf{q} = \begin{bmatrix} q_1 \\ q_2 \\ \vdots \\ q_n \end{bmatrix}, \quad \mathbf{X} = \begin{bmatrix} X_1 & 0 & 0 & \cdots & 0 & 0 \\ X_2 & X_1 & 0 & \cdots & 0 & 0 \\ X_3 & X_2 & X_1 & \cdots & 0 & 0 \\ \vdots & \vdots & \vdots & & \vdots & \vdots \\ X_n & X_{n-1} & X_{n-2} & \cdots & X_2 & X_1 \end{bmatrix} \tag{21}$$

The components of this matrix are related to the constant and triangular basis function cases by

$$\text{Piece-wise constant basis-function cases: } X_i = \Delta \phi_{i-1} \tag{22}$$

$$\text{Triangular basis-function cases: } X_i = \delta^2 \eta_{i-1}$$

A matrix that is needed in the Tikhonov regularization method is

$$\mathbf{X}^T \mathbf{X} = \begin{bmatrix} \sum_{i=1}^n X_i^2 & \sum_{i=1}^{n-1} X_i X_{i+1} & \sum_{i=1}^{n-2} X_i X_{i+2} & \cdots & X_1 X_n \\ \sum_{i=1}^{n-1} X_i X_{i+1} & \sum_{i=1}^{n-1} X_i^2 & \sum_{i=1}^{n-2} X_i X_{i+1} & \cdots & X_1 X_{n-1} \\ \vdots & \vdots & \vdots & & \vdots \\ X_1 X_n & X_1 X_{n-1} & X_1 X_{n-2} & \cdots & X_1^2 \end{bmatrix} \tag{23}$$

Notice that this is a symmetric matrix.

It can be helpful to examine the basis-function case components as a function of time. Figure 2 shows dimensionless values as a function of dimensionless time for  $\alpha \Delta t / b^2 = \alpha t_0 / b^2 = 0.024$ . The curve labeled "1"

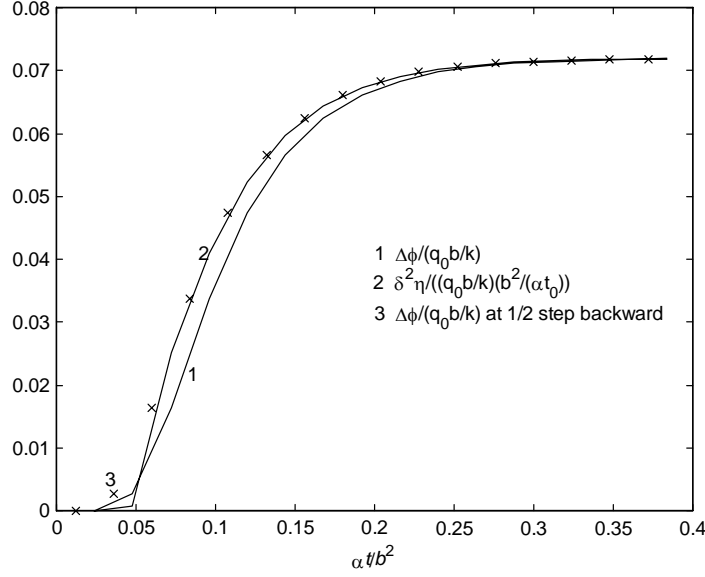


Figure 2. Constant and triangular basis-function case components,  $\alpha t / b^2 = 0.024$ .

is  $\Delta\phi_i / (q_0 b / k)$  and the curve labeled “2” is  $\delta^2\eta / [(q_0 b / k)(b^2 / \alpha t_0)]$ . The surprising point is that the piece-wise constant basis-function case curve is similar to the triangular basis function curve if it is plotted at  $1/2$  time step backward, that is, 0.012; see the “x” points, labeled curve 3 in Figure 2. That makes sense because  $\Delta\phi_i$  is a forward difference approximation and is more accurate at the midpoint of the interval. If a smaller dimensionless time step such as  $\alpha\Delta t / b^2 = 0.012$  is used, the overlapping of these two curves is almost complete. (See the relation between the two  $T$  histories mentioned below eqn. (10b).) Relative to estimation of the surface heat flux, the piece-wise constant and triangular basis function solutions using Tikhonov regularization should give very nearly the same results if the piece-wise constant basis function results are offset backward  $1/2$  of the time step. Consequently only the triangular basis-function approximation for Tikhonov regularization is considered in this paper.

A couple more points are made regarding Figure 2. First, shapes of the curves for various time steps of  $\Delta t$  (which we also set equal to  $t_0$ ) are the same for small dimensionless times. Second, the magnitude is directly proportional to  $\Delta t$ . Consider eqn. (8b) for sufficiently large times such that the summation has disappeared (which according to Figure 2 is about  $\alpha\Delta t / b^2 = 0.25$ ). Then using eqn. (8b) we can write

$$\left. \frac{T(0, t_{i+1}) - T(0, t_i)}{q_0 b / k} \right|_{\alpha t / b^2 > 0.25} \approx 3 \frac{\alpha(t_{i+1} - t_i)}{b^2} = 3 \frac{\alpha\Delta t}{b^2} \approx \left. \frac{\Delta\phi_i}{q_0 b / k} \right|_{\alpha t / b^2 > 0.25, q_0 = 1} \quad (24)$$

Hence the magnitude of the constant basis functions is directly proportional to  $\Delta t$ . Notice for  $\alpha\Delta t / b^2 = 0.024$ , which is used in Figure 2, that the value given by eqn. (24) is 0.072 which is maximum value shown in Figure 2. Using the second difference of  $\eta$  as defined by eqn. (15) and eqn. (10b) yields exactly the same result.

Now from eqn. (22) the  $\Delta\phi_i$  and  $\delta^2\eta_i$  values are simply related to the  $X_i$  components in the sensitivity matrix given by eqn. (21). For sufficiently large dimensionless times, some terms in eqn. (23) are simply related to one another. For example, for  $\alpha N\Delta t / b^2$  greater than about 0.25, diagonal elements can be given by

$$\sum_{i=1}^I X_i^2 = \sum_{i=1}^N X_i^2 + (I - N)X_N^2 = \sum_{i=1}^N X_i^2 + (I - N) \left( \frac{b}{k} 3 \frac{\alpha\Delta t}{b^2} \right)^2, \quad I > N \quad (25)$$

In zeroth order Tikhonov regularization [2], the sum of squares function

$$S = (\mathbf{Y} - \mathbf{T})^T (\mathbf{Y} - \mathbf{T}) + \alpha_\tau \mathbf{q}^T \mathbf{q} = (\mathbf{Y} - \mathbf{X}\mathbf{q})^T (\mathbf{Y} - \mathbf{X}\mathbf{q}) + \alpha_\tau \mathbf{q}^T \mathbf{q} \quad (26)$$

is minimized with respect to the parameter vector  $\mathbf{q}$ . The symbol  $\mathbf{Y}$  is the measurement vector and the initial temperature is zero. The  $\alpha_\tau$  symbol is the Tikhonov regularization parameter; it is discussed in more detail in [2]. The estimated value heat flux vector, denoted  $\hat{\mathbf{q}}$ , is then given by

$$\hat{\mathbf{q}} = [\mathbf{X}^T \mathbf{X} + \alpha_\tau \mathbf{I}]^{-1} \mathbf{X}^T \mathbf{Y} \quad (27)$$

It is important to observe that eqn. (27) is a linear function of the measurements temperature vector  $\mathbf{Y}$ .

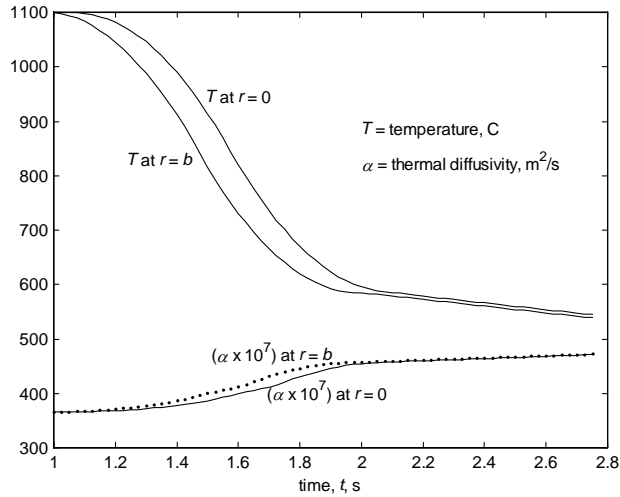


Figure 3. Temperatures and thermal diffusivities at  $r = 0$  and  $b$  for the solid tungsten ball example.

### 3.3 Filter Coefficients

The IHCP estimation equations, (eqns (11), (19) and (27)), are linear functions of the measurements and can be used to obtain the filter coefficients. In each case the filter coefficients are found by setting all the components of  $\mathbf{Y}$  equal to zero except one which is set equal to unity.

The filter coefficients calculated using the filter equation given by eqn. (1) can be written as

$$\begin{aligned} \hat{q}_M &= \sum_{j=1}^{m_o+m_f} f_j Y_{m_f+M-j} = \sum_{j=1}^{m_f} f_j Y_{m_f+M-j} + \sum_{j=m_f+1}^{m_o+m_f} f_j Y_{m_f+M-j} \\ &= (f_1 Y_{m_f+M-1} + f_2 Y_{m_f+M-2} + \dots + f_{m_f-1} Y_{M+1} + f_{m_f} Y_M) + (f_{m_f+1} Y_{M-1} + \dots + f_{m_o+m_f} Y_{M-m_p}) \end{aligned} \quad (28)$$

Consider now the function specification method and let  $m_f = r_f$ , the number of future time steps. Also let all

$$Y_i = 0 \text{ for all } i \text{ except } Y_{r_f} = 1 \quad (29)$$

Then the heat flux components are calculated using the appropriate algorithm, such as eqns (11) or (19). The heat flux components are then known for this special case. Setting  $M = 1$  in eqn. (28) then yields

$$\hat{q}_1 = f_1 Y_{r_f} + 0 = f_1 \cdot 1 = f_1, \quad f_1 = \hat{q}_1 \quad (30)$$

and setting  $M = 2$  and again using eqn. (28) gives  $f_2 = \hat{q}_2$ . More generally we obtain

$$f_j = \hat{q}_j, \quad j = 1, 2, \dots, m_p + m_f \quad (31)$$

Basically the same procedure is followed to get the filter coefficients using the Tikhonov regularization equation given by eqn. (27).

## 4. EXAMPLE

### 4.1. Description

An example of a solid tungsten ball with a radius of  $b = 0.005$  m is considered. It is initially at  $1100$  °C and quenched in a fluid. The heat flux leaving the tungsten ball is known as a function of time and is given by four straight lines. From  $t = 0$  to  $1$  s the heat flux is zero; the  $q$  then decreases to  $-4,800,000$  W/m<sup>2</sup> at  $1.5$  s;  $q$  then increases to  $-300,000$  W/m<sup>2</sup> at  $2$  s; and  $q$  then increases to  $-180,000$  W/m<sup>2</sup> at  $8$  s. This is shown in the last figure, Figure 7. The measurement time step is  $0.025$  s. The temperature-dependent thermal properties are taken from Incropera and DeWitt [4] and are given in the below table.

Temperature, °C	Thermal conductivity, $k$ , W/m·C	Thermal diffusivity, $\alpha$ , m <sup>2</sup> /s
527	125	0.0000447
727	118	0.0000413
927	113	0.0000385
1227	107	0.0000353

Temperatures generated using the above information are shown in Figure 3. The temperature drops about  $500$  °C in one second and the maximum temperature from the center to outer radius is about  $100$  °C. The maximum

temperature gradient is 425 °C /cm. See also the lowest two curves in Figure 3 which show that the increase in the thermal diffusivity is from about 366E-7 m<sup>2</sup>/s at 1100 °C to 460E-7 m<sup>2</sup>/s at 600 °C, a 25% increase.

#### 4.2. Filter Coefficients

The filter coefficients are found as described above. Only one  $Y$  value is set equal to unity and all the others are set to zero. The index  $i$  for setting  $Y_i = 1$  can be any value in the midrange, it should not be near the beginning nor near the end. Although only one  $Y$  value equal to 1 is needed, four are used in Figure 4 to illustrate that very nearly the same filter coefficients are obtained for all locations of setting  $Y = 1$  except those near the beginning and the end of the time interval. The curves in Figure 4 are for  $Y = 1$  at the times of 0.1, 0.8, 1.6 and 2.4 seconds, corresponding to the 4<sup>th</sup>, 32<sup>th</sup>, 64<sup>th</sup> and 96<sup>th</sup> times, respectively. The curve for  $Y_4 = 1$  is anomalous since the filter coefficients are much smaller than the other cases. The filter coefficients are the same in this example for  $Y_n = 1$  for about  $n$  starting at  $r_f = 6$  up to about 10 steps before the final time. The coefficients can be found from any one of the curves in Figure 4 except the first one.

The curves shown in Figure 4 are for the function specification filter coefficients for the linear basis-function algorithm, eqn. (19), for  $r_f = 6$  future times for the 927°C tungsten properties; the dimensionless time step is  $\alpha\Delta t / b^2 = 0.0385$ . This is such a small dimensionless time step that negligible information regarding the heated surface is obtained in one time step; see Figure 2. In 6 time steps, the dimensionless time covered is 0.231 at which time Figure 2 reveals that a great deal of information regarding the heated surface is obtained; this is reflected by the filter coefficients shown in Figure 4.

Basically the same procedure is followed to get the filter coefficients using the Tikhonov regularization equation given by eqn. (27). See Figure 5 which shows the Tikhonov filter coefficients for this tungsten example with measurements of 0.025 s time steps, linear basis functions, properties evaluated at 927 °C, and zeroth order Tikhonov regularization parameter value of  $\alpha_T = 10^{-10} \text{C}^2 \cdot \text{s}^2/\text{m}^4$ . Although only one  $Y=1$  is needed to obtain the filter coefficients, five curves are shown ( $Y=1$  at  $t = 0.05, 0.8, 1.6, 2.4$  and  $3.375$ ). Again we note that the mid-range of filter coefficients are the same in value, those  $Y=1$  at  $t = 0.8, 1.6$  and  $2.4$  in Figure 5, but the beginning and end values are different; hence calculation at the beginning times should use data about 0.3 s (in this example) before the first heat flux of interest. Heat fluxes should not be estimated near the end of the data.

The filter coefficient curves shown in Figs. 4 and 5 are derived using quite different IHCP algorithms yet are quite similar. (They could be made even more similar by adjusting the regularization parameters for each method which are  $r_f$  and  $\alpha_T$ .) The characteristics of these curves are important and now considered. There is an anticipatory quality; the  $t = 0.8$  s curve of Figure 5, for example, shows a rise about 0.45 s which is well before the  $Y$ -impulse at 0.8 s. At the time step before 0.8 s, namely 0.775 s, the filter coefficient abruptly drops to a minimum value. The magnitudes of the filter coefficients can provide insight into the effects of measurement errors. For an example Figure 5 is used; an error of 1°C can first cause an error in the surface heat flux of about +10,000 W/m<sup>2</sup> followed shortly thereafter with an error of about -14,000 W/m<sup>2</sup>. These error values should be compared with the temperatures and heat fluxes in the example. From Figure 3, the maximum temperature is 1100 °C and the maximum temperature drop across the ball is about 100°C. It is not unreasonable to expect temperatures measured to have errors about 10°C in this case. The maximum heat flux magnitude in the example is 4,800,000 so an error of 10 times 14,000 = 140,000 (or 3% of the maximum value) would not be unsatisfactory. However, when the heat flux is down to about 300,000, an error of 140,000 may not be satisfactory.

Another point relates to the duration of non-zero values of the filter coefficients, which in symbols is the value of  $(m_p + m_f)\Delta t$ ; it is about 0.5 s in Figure 5 but the region where the changes of  $f_j$  are the greatest is only about 0.25 s. In this latter time period the thermal diffusivity at  $r = 0$  changes only 9%. Fortunately the effects upon the heat flux of such property changes are not large compared to the effects of temperature measurement errors or regularization. See Figure 6 which shows the filter coefficients for 527, 927 and 1227 °C. The duration of non-zero filter values is about the same in each case. Moreover one can infer from Figure 6 that linear interpolation in temperature of the filter coefficients is appropriate.

#### 4.3. Numerical values

Values of the heat flux for the example using 0<sup>th</sup> order Tikhonov regularization are shown in Figure 7 with  $\alpha_T = 10^{-10} \text{C}^2 \cdot \text{s}^2/\text{m}^4$ , time steps of 0.025 s and the properties evaluated at 927 °C. The exact heat flux values are depicted by the solid straight lines and the estimated heat flux values by the dots. The heat flux is slightly delayed compared to the exact values but the direct use of the whole domain Tikhonov regularization method gives nearly the same results when the thermal properties are evaluated at 927 °C. The heat flux estimate at time 1.25 s in Figure 7 is -2,209,000 W/m<sup>2</sup>, compared to the true value of -2,400,000 W/m<sup>2</sup>.

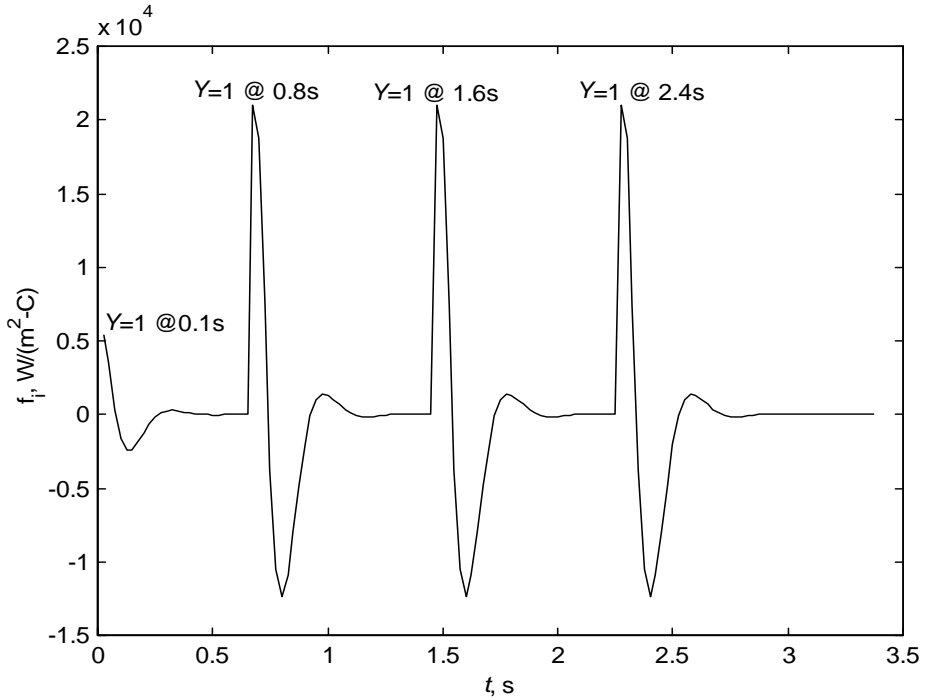


Figure 4. Function specification filter coefficients for solid sphere of tungsten.  $r_f = 6$ ,  $\Delta t = 0.025$  s.  $Y = 1$  at 0.1 s, 0.8 s, 1.6 s and 2.4 s, or time index of  $M = 4, 32, 64$  and 96. Any one of the last three filter coefficient curves can be used.

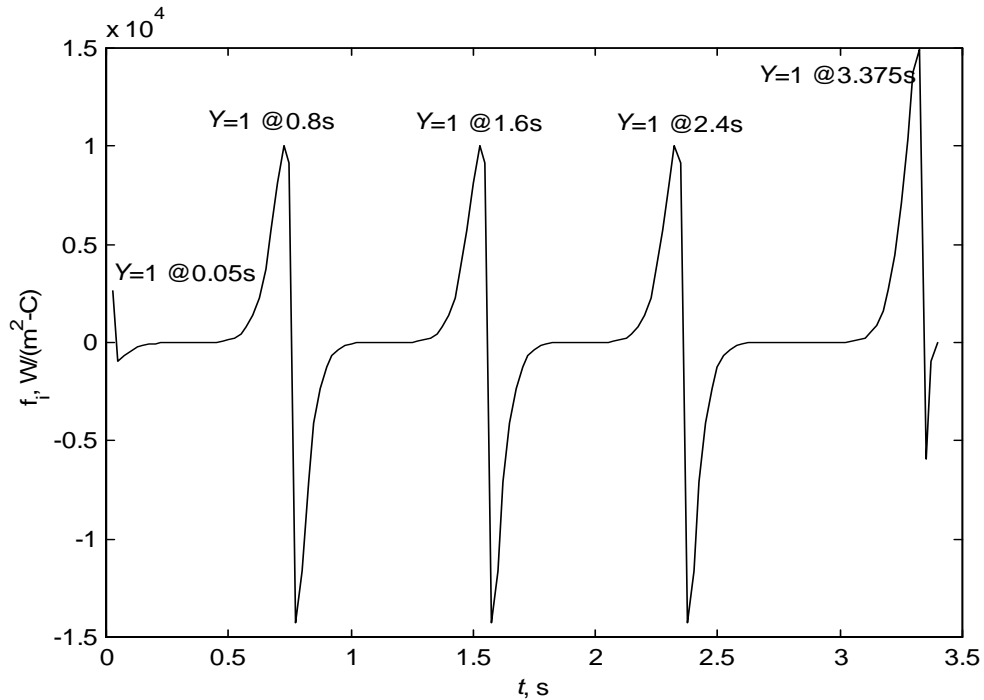


Figure 5. Tikhonov 0<sup>th</sup> order filter coefficients for tungsten example,  $\Delta t = 0.025$  s,  $\alpha_T = 1.0E-10$   $C^2 \cdot s^2/m^4$ , triangular basis functions. Properties at 927 °C.  $Y = 1$  at  $t = 0.05, 0.8, 1.6, 2.4$  and 3.375 s. Any one of the three middle curves can be used.



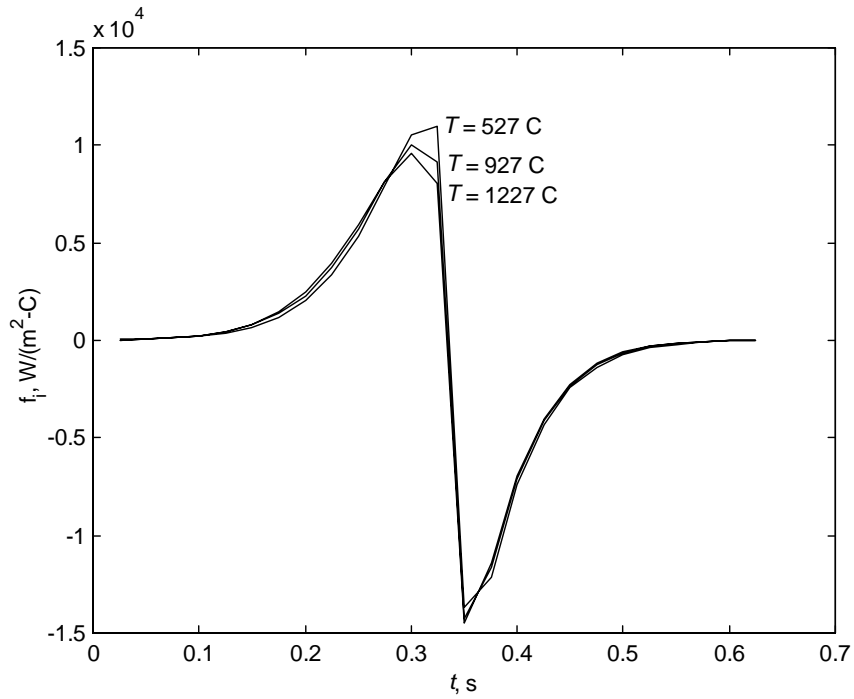


Figure 6. Tikhonov 0<sup>th</sup> order filter coefficients for tungsten ball example for properties at 527, 927 and 1227 °C,  $Y = 1$  at  $t = 0.375$  s.  $\Delta t = 0.025$  s,  $\alpha_T = 1.0E-10 C^2 \cdot s^2/m^4$ , triangular heat flux basis functions.

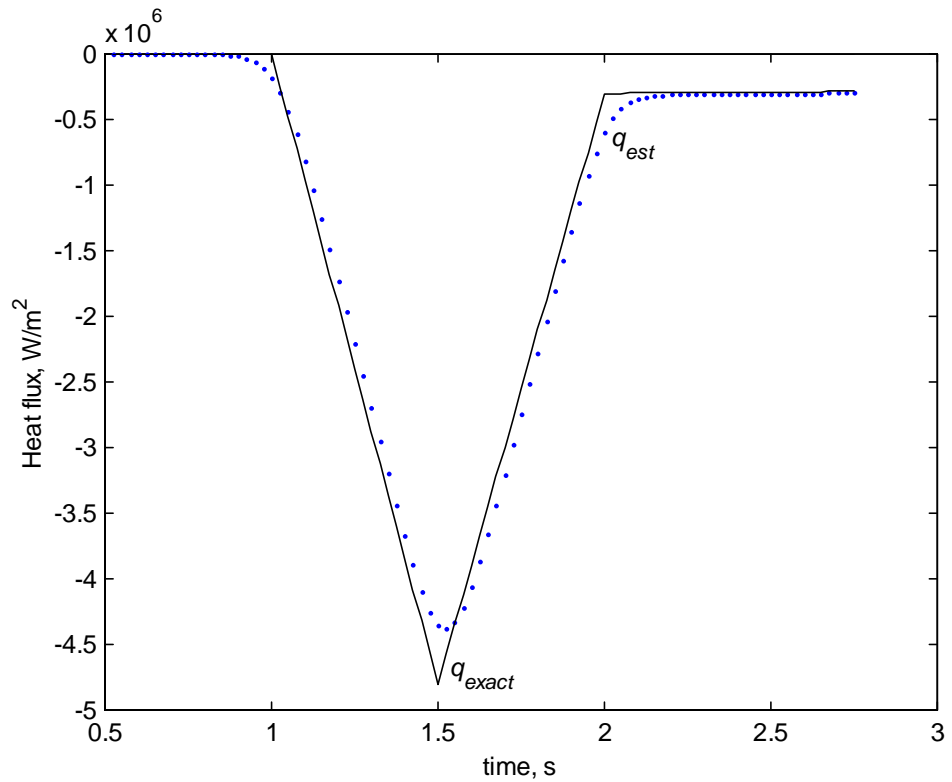


Figure 7. Estimated heat flux using the filter algorithm with the coefficients coming from the Tikhonov 0<sup>th</sup> order algorithm with  $\Delta t = 0.025$  s,  $\alpha_T = 1.0E-10 C^2 \cdot s^2/m^4$ , triangular heat flux basis functions. Properties at 927 C.

The errors at the times of 1.25, 1.5, 1.75 and 2.75 s are respectively, 191,000, 441,000, -197,000 and -11,970 W/m<sup>2</sup>; the magnitudes of these errors are 8.0%, 9.2%, 8.2% and 4.2% relative to the respective exact values. If the same procedure is repeated with the thermal properties evaluated at 527 °C, the corresponding errors are 352,000, 651,000, -118,000 and -2206 W/m<sup>2</sup>, which are 15%, 14%, 4.9% and 0.8% in magnitude error compared to the exact values. This reveals that the heat fluxes are more accurate at the beginning times using properties evaluated at 927 °C.

The errors in estimating the heat flux are not mainly caused by the approximate analysis for the  $T$ -dependent thermal properties. The regularization procedure itself causes the major error but the temperature at which the properties are evaluated is also important. The temperature at  $r = 0$  at 1.25 s is 1066.8 C and the associated thermal properties are  $k = 110$  W/m·C and  $\alpha = 0.0000369$  m<sup>2</sup>/s. Consider three different exact analyses for estimating the heat flux at time 1.25 s. Using this exact “data,” the whole domain Tikhonov method yields the heat flux value of 2,248,000 W/m<sup>2</sup>. If the filter analysis is used with this same data, the heat flux of about 2,242,000 W/m<sup>2</sup> is found, a difference about -0.3%. If the filter analysis (with the coefficients the same as those used to get the 2,242,000 value) is used for the temperatures calculated using the  $T$ -dependent thermal properties, the result is 2,270,000 W/m<sup>2</sup>, about 0.98% larger than 2,248,000. Since each of these estimates is about 6% low compared to the correct value of 2,400,000 W/m<sup>2</sup>, the major error is caused by the regularization, not the treatment of the temperature variation of the thermal properties.

## 5. CONCLUSIONS

For the case of a spherical tungsten ball dropped into a cooling fluid, the heat flux leaving the ball is very large, resulting in the temperature dropping rapidly. The temperature gradients are also large in the ball, up to 425 K/cm. The calculation of the heat flux in such cases is usually done with a nonlinear IHCP analysis to treat the temperature-dependent thermal properties. This paper demonstrates that a linear filter-type analysis can be used to estimate the heat flux from transient temperature measurements in such cases. Such an analysis can be very efficient for similar experiments that are repeated often and could even be part of the software associated with a heat flux measuring instrument. Many other repetitive experiments can utilize this filter analysis procedure.

The IHCP filter method can be extended to many other geometries and problems. It is particularly appropriate for continuous manufacturing processes that have periodic heating and cooling. The most technically-demanding aspects of determining the heat flux can be relegated to experts to determine the filter coefficients for a specific production problem. Then these filter coefficients can be applied without specific expertise, such as knowledge of the numerical solution of the transient heat conduction problem, selection of a regularizing method and selection of regularizing parameters.

## Acknowledgement

The author would like to express appreciation to Dr. Arafa Osman for carefully reading this paper and making many significant comments.

## REFERENCES

1. J.V. Beck, Determination of undisturbed temperatures from thermocouple measurements using correction kernels, *Nuclear Eng. and Design* (1968) **7**, 170-178.
2. J.V. Beck, B. Blackwell and C.R. St. Clair, *Inverse Heat Conduction, Ill-Posed Problems*, Wiley-Interscience, NY, 1985.
3. J.V. Beck, K.D. Cole, A. Haji-Sheikh and B. Litkouhi, *Heat Conduction Using Green's Functions*, Hemisphere Publishing Company, Washington, DC, 1992.
4. F.P. Incropera and D.P. DeWitt, *Introduction to Heat Transfer*, 3<sup>rd</sup> Ed., Wiley, 1996.
5. D.A. Murio, *The Mollification Method and the Numerical Solution of Ill-Posed Problems*, Wiley-Interscience, NY, 1993.
6. M.N. Ozisik and H.R.B. Orlande, *Inverse Heat Transfer*, Taylor & Francis, NY, 2000.
7. A.N. Tikhonov and V.Y. Arsenin, *Solutions of Ill-Posed Problems*, Winston/Wiley, NY, 1977.
8. K.A. Woodbury, *Inverse Engineering Handbook*, CRC Press, Boca Raton, 2003.